Journal of Catalysis **182,** 234–243 (1999)
Article ID jcat.1998.2350, available online at http://www.idealibrary.com on IDEAL®

An Investigation into the Reactivity, Deactivation, and in Situ Regeneration of Pt-Based Catalysts for the Selective Reduction of NO_x under Lean Burn Conditions

R. Burch, P. Fornasiero, and B. W. L. Southward

Catalysis Research Centre, Department of Chemistry, University of Reading, Whiteknights, Reading, RG6 6AD, United Kingdom

Received September 8, 1998; revised November 9, 1998; accepted November 9, 1998

The activity and deactivation characteristics of Pt-based lean burn De-NO_x catalysts have been investigated and the relationships between temperature, nature of reductant (*n*-octane) and NO_2 concentrations, and the mechanism(s) of deactivation have been examined. The effects of Pt loading and particle size on the activity and deactivation have also been studied. The results show that deactivation of the catalyst is due to site blocking via an unidentified carbonaceous deposit and that the initial surface state of the Pt is crucial. In all cases clean Pt surfaces were found to display an initial period of surprisingly high activity prior to deactivation, the rate of which was inversely related to reaction temperature. Deactivation is proposed to arise from a combination of factors which inhibit adsorption and reaction of *n*-octane, due to encroachment onto the Pt surface of hydrocarbonaceous species accumulating initially on the support in the vicinity of the Pt/support interface. It is possible that these carbon-containing deposits comprise some form of organonitrogen species. The loss of activity due to this gradual encroachment results in a reduction in the temperature of the Pt particles, leading to a further decrease in reaction and/or desorption rates, and rapid deactivation then ensues. The use of higher Pt loadings leads to enhanced activity at lower temperatures and increased tolerance to the deactivating effects of surface deposition. Catalyst activity and tolerance to deactivation were further enhanced by controlled sintering, which, within certain limits, resulted in excellent, stable low-temperature De-NO_x activity. The divergent activity of SiO_2-, Al_2O_3-, and ZrO_2-based catalysts reflects support effect contributions, with the former displaying poor low temperature activity and rapid deactivation while the latter supports, particularly ZrO_2, exhibited high De-NO_x activity at lower temperatures without deactivation. The use of temperature "spiking" and micropulse injection techniques facilitated regeneration of the full De-NO_x activity. In particular, the use of micropulse injections of CH_3OH into the *n*-C_8H_{18}–O_2–NO reaction completely circumvented deactivation and demonstrated the potential for obtaining very high NO_x conversions at low temperatures.

Key Words: **De-NO_x; catalyst; Pt; octane; lean burn; deactivation; reactivation.**

1. INTRODUCTION

Within the framework of increasingly stringent emissions control legislation it is apparent that diesel engines will soon require exhaust control technology comparable to that afforded to the petrol engine by use of the stoichiometric catalytic converter (1–3). However, despite intensive research into the field of De-NO_x under fuel lean conditions (4–41), to date there has been no suitable material developed that will attain the high levels of activity required under typical diesel engine operation. The problems encountered have been manifold, ranging from poisoning of the active materials by SO_x derived from the combustion of fuel-bound sulfur or engine lubricants to problems of hydrothermal instability under the high partial pressures of steam in the exhaust. These problems have been particularly pronounced for the various zeolitic catalysts suggested to date, as has the sintering/migration in the zeolite or over reduction of the active metal sites under reaction conditions (2, 5–7, 14). One promising field of investigation has been found in the study of Pt-based catalysts, which display high hydrothermal stability and a greater tolerance to SO_x, and which do not suffer from serious deactivation due to metal sintering (1, 6, 8, 12–15).

However, even under ideal conditions there are still fundamental problems to be addressed before the successful commercial application of these catalysts can be realised. A primary goal is high De-NO_x activity at low temperatures, typical of "cold start" or "urban cycle" conditions, without deactivation. This problem is highlighted by the observation of NO_x emissions at exhaust catalyst temperatures as low as 120°C (1), prompting further legislation to cover low-temperature emissions (2). To achieve this end we have examined the roles of temperature, reaction intermediate concentrations, metal loading/dispersion, and metal–support effects in achieving and maintaining high De-NO_x activity. The presence and identity of those species responsible for deactivation have also been probed by in situ and ex-situ analyses. Finally, attempts have been made to circumvent the mechanism of deactivation to enable high activity to be achieved at lower temperatures.

2. EXPERIMENTAL

All catalysts used were prepared by incipient wetness impregnation of the dried supports (Azko CK300 Al_2O_3,

0021-9517/99 $30.00

Grace 432 silica, and ZrO_2 ex melcat X20 632/03 $Zr(OH)_2$) using platinum dinitrodiammine precursor (ex Johnson Matthey) to give nominal Pt loadings of 1%. The exception to this was the commercially available catalyst, 0.3% Pt-Al_2O_3 (ex Azko). Catalyst testing was performed in a quartz tubular downflow reactor (i.d. 5 mm). The sample (100 mg, 250–850 μm) was held between plugs of quartz wool. An upstream bed of quartz was used as a preheater and a thermocouple was located in the centre of the catalyst bed. The reactor was heated using a Eurotherm 8000 series controlled furnace, with furnace temperatures being maintained to $\pm 1^\circ$C. The reactant gases, NO, NO_2, C_3H_6, and O_2, and the carrier, He, were fed from independent mass flow controllers while *n*-octane was added using an Instech model 2000 syringe pump. All reactor lines were trace-heated (120°C) to prevent condensation. Unless otherwise stated, the total flow was 200 cm^3 min^{-1}, with a feed composition of 4000 ppm C, 500 ppm NO, and 5% O_2 in He (standard reaction mixture). The NO and total NO_x were determined by a Signal series 4000 chemiluminesence detector and CO_2 analysis performed using a Signal series 2000 IR CO_2 analyser. GC analysis was carried out using a Perkin–Elmer Autosystem GC, equipped with TCD and FID detectors. Product separation was achieved using heysep N and molecular sieve 5A columns equipped with back flush. No reaction was observed over quartz wool below 500°C. No CO formation was detected during De-NO_x over the range of temperatures investigated. In these studies NO_x conversion is defined as the reduction of NO and NO_2 to N_2 and N_2O.

Prior to reaction, catalysts were aged overnight at 550°C in standard reaction mixture to remove adsorbed species and eliminate residues from the Pt precursor. In subsequent studies the catalyst was then "cleaned," viz. calcined at 550°C in 5% O_2/He for 1 h. This was to ensure removal of any retained surface species. In all profile experiments, the temperature was increased stepwise and held until steady-state activity was obtained (typically 30 min).

Temperature-programmed oxidations (TPO) and desorptions (TPD) were performed in situ using the equipment described above, over the range 100 to 550°C at a ramp of 10°C min^{-1}. All samples were purged for 30 min in He prior to analysis. NO_x and CO_2 concentrations were monitored every 0.1 min via a PC interface while N_2, N_2O, and hydrocarbon concentrations were analysed by GC every 30 min. Analysis of adsorbates was performed by dosing clean samples at 198°C for 10 min in reactant flow (see main text), followed by a 15 min He purge (200 cm^3 min^{-1}). All samples were then cooled in flowing He for 100 min prior to TPO analysis.

Hydrogen chemisorption was performed by evacuating the sample at 300°C for 30 min, followed by static reduction in H_2 (0.5 atm) for 30 min, again at 300°C. The sample was then re-evacuated at 300°C for 2 h and cooled under vacuum to room temperature. A dosing equilibration time of 10 min was employed. The adsorbed volumes were determined by extrapolation to zero pressure of the linear part of the adsorption isotherm and dispersion obtained by assuming a chemisorption stoichiometry of H : Pt = 1.0. Pt particle diameters were calculated assuming spherical geometry. BET surface areas were determined by N_2 adsorption using apparatus built in-house. Infrared analysis was performed using a PC-interfaced Perkin–Elmer 1720-X FT spectrometer. Data acquisition was performed in the transmission mode (TGS detector) at 4 cm^{-1} resolution using I-R Data Manager software.

3. RESULTS

(1) H_2 Chemisorption, Particle Size, and Surface Area Analyses

Table 1 details various physical characteristics of samples used in this study. The hydrogen chemisorption shows that the catalysts had a range of Pt particle sizes. Attempts to analyse used catalysts by chemisorption yielded uncertain results. In all cases the H_2 uptake was low, presumably due to poisoning of the Pt. Clearly, the deposits formed during reaction were not removed by the static reduction treatment.

(2) Microreactor Studies of the Activity and Deactivation of 0.3% Pt/Al_2O_3

Initial studies were concentrated upon an examination of the 0.3% Pt/Al_2O_3 catalyst in order to standardise the many variables affecting activity. Subsequent experiments were then broadened to encompass other factors such as Pt loading and support effects. The results presented show the general trends observed but are representative of a much larger body of information.

The effect of temperature on the *n*-C_8H_{18}–NO–O_2 reaction is shown in Fig. 1. The conversion of *n*-C_8H_{18} and NO commenced simultaneously and increased with temperature until 100% *n*-C_8H_{18} conversion was attained. The maximum NO conversion was 87% at 220°C, the major product being N_2 (60%), although N_2O was also produced. Above this temperature NO conversion decreases, and NO is replaced by increasing amounts of NO_2, the latter peaking at ca. 370°C. Similar trends have been observed for the reaction of C_3H_6–NO–O_2 over supported Pt (14, 16–18) and are considered to be associated with NO dissociation on a Pt surface covered by C_3H_6-derived species (16). These data contrast with the homogeneous reaction between *n*-octane and O_2, which did not occur below 200°C, and the combustion over Al_2O_3, where only 2% conversion was recorded at 300°C. These observations confirm that both the combustion and the De-NO_x reactions are associated with the presence of Pt moieties.

TABLE 1

H_2 Chemisorption and Surface Area Data for Supported Pt Catalysts

Sample	Pt loading (%)[a]	Pretreatment[b] gas/temp (°C)/time (h)	H/*M*	Metal SA ($m^2\ g^{-1}$)	Particle ∅ (nm)[c]	BET ($m^2\ g^{-1}$)
Pt/Al_2O_3	0.3	O_2–He/550/1	0.37	0.27	3.1	195
Pt/Al_2O_3	0.3	*n*-C_8H_{18}–NO–O_2/198/3	0.10	0.07	[d]	
Pt/Al_2O_3	0.3	*n*-C_8H_{18}–NO–O_2/223/3	0.28	0.21	[d]	
Pt/Al_2O_3	1	O_2–He/550/1	0.36	0.89	3.1	218
Pt/Al_2O_3	1	*n*-C_8H_{18}–NO–O_2/175/3	0.12	0.3	[d]	
Pt/Al_2O_3	1	O_2–He/700/15	0.28	0.68	4.1	
Pt/Al_2O_3	1	O_2–He/740/24	0.10	0.24	12	
Pt/SiO_2	1	O_2–He/550/1	0.18	0.45	6.2	265
Pt/SiO_2	1	*n*-C_8H_{18}–NO–O_2/175/3	0.06	0.14	[d]	
Pt/ZrO_2	1	O_2–He/550/1	0.06	0.07	38	12
Pt/ZrO_2	1	*n*-C_8H_{18}–NO–O_2/175/3	0.01	0.01	[d]	

[a] Nominal metal loading.
[b] All samples first pretreated at 550°C in 500 ppm *n*-C_8H_{18}/500 ppm NO/5% O_2.
[c] Average particle diameter calculated from the H_2 chemisorption assuming spherical geometry.
[d] The presence of "coke" on the surface does not allow the particle diameter to be estimated from H_2 chemisorption.

As detailed previously, each point in Fig. 1 corresponds to steady-state activity. However, it was found that below the hydrocarbon light-off temperature (defined as corresponding to 20% conversion of octane, Fig. 1), the catalyst exhibited significant deactivation, with hydrocarbon and NO_x conversions decreasing with time (Fig. 2, Trace 1). Conversely, no deactivation was noted above the light-off temperature (Fig. 2, Trace 4). Since Trace 1 corresponds to the deactivation occurring at 198°C on a catalyst preexposed to reaction mixture at lower temperatures, it was necessary to examine the activity of a clean catalyst at 198°C (Fig. 2, Trace 2). Surprisingly it was found that the catalyst displayed an initial period of high activity (ca. 2 h), with an associated combustion exotherm, before both decreased over a period of 1 h to a final NO_x conversion of ca. 10%.

This is an important result and indicates that previous data concerning the activity of Pt-based De-NO_x catalysts are potentially unrepresentative since they may only reflect the activity of surfaces poisoned at lower temperatures. This effect is particularly relevant to real diesel exhaust conditions since further data (see later) indicate that hydrocarbon retention effects become increasingly significant with increased hydrocarbon chain length. Hence

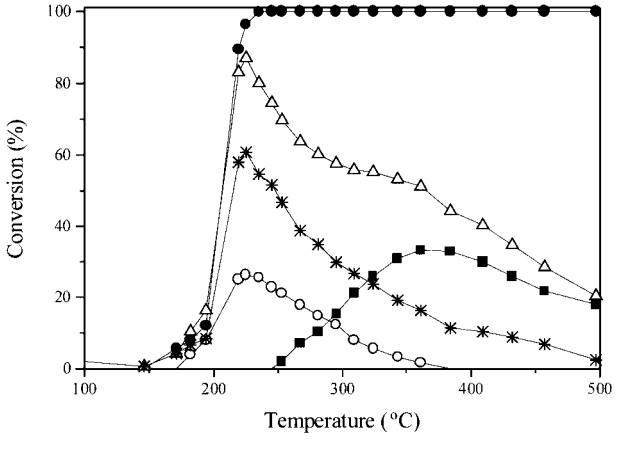

FIG. 1. The effect of temperature on the *n*-C_8H_{18}–NO–O_2 reaction over 0.3% Pt/Al_2O_3. Reactant feed: 500 ppm *n*-C_8H_{18}, 500 ppm of NO and 5% O_2 in He. (Conversion of (●) *n*-C_8H_{18} to CO_2, (Δ) NO (to $N_2 + N_2O$), (∗) NO to N_2, (○) NO to N_2O, and (■) NO to NO_2.)

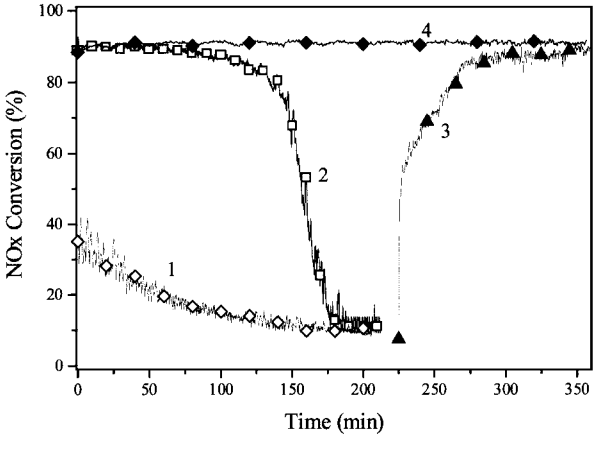

FIG. 2. Comparison of De-NO_x activity over 0.3% Pt/Al_2O_3: (1, ◇) at 198°C after exposure to reaction mixture at lower temperatures; (2, □) clean catalyst at 198°C; (3, ▲) reaction at 223°C for a catalyst previously deactivated at 198°C; (4, ◆) reaction of a clean catalyst 223°C. Reaction feed as in Fig. 1.

n-octane is more toxic at lower temperatures than propane (see TPO data later).

Figure 2, Trace 3, shows the effect of increasing the furnace temperature from 198 to 223°C after the reaction reported in Fig. 2, Trace 2. It was found that upon increasing the temperature the activity of the deactivated catalyst increased sharply for the first hour (cf. ca. 5 min. for the furnace to stabilise at 223°C). In the next 2 h the activity increased slowly up to the value observed for a clean catalyst. (Note: the activity of the catalyst was measured for a further 7 h without deactivation.) These experiments showed that the deactivation process could be reversed.

To further investigate the role of surface poisoning, a clean catalyst was pretreated in *n*-C_8H_{18} (500 ppm) and O_2 (5%) (i.e., without NO) at 198°C for 3 h. Hydrocarbon conversion, as determined by GC analysis, was complete. However, CO_2 production varied with time on stream. At the end of 3 h the sample was cooled and a TPO experiment performed. This sample showed a CO_2 peak at ca. 400°C, indicative of the removal of carbon-containing material from the catalyst (row 1, Table 2). In a second, separate experiment 0.3% Pt/Al_2O_3 was again utilised for an *n*-octane combustion (*n*-C_8H_{18} (500 ppm) and O_2 (5%)). However, in this case, the catalyst was utilised in a standard de-NO_x reaction at 198°C (Fig. 3, Trace 2). The activity measured was considerably lower than that of the clean catalyst. This confirmed that deactivation could occur at these low temperatures because of retained hydrocarbon-derived species formed even when *n*-C_8H_{18} is reacted in a large excess of O_2.

NO_2 can react with hydrocarbonaceous moities so we have examined the possible influence of NO_2 on the extent of deactivation. Three NO_2 pretreatments were investigated. First, the catalyst was exposed to a mixture of NO (500 ppm) and O_2 (5%) for 1 h prior to reaction (Fig. 3, Trace 3). Second, a fresh catalyst was treated with a mixture of NO_2 (420 ppm) and O_2 (5%) for 2 h (Fig. 3, Trace 4). Finally the effect of cofed NO_2 on activity was examined (Fig. 3, Trace 5).

The first pretreatment generated NO_2 in situ by reaction of NO with O_2 on the Pt with a significant adsorption of NO_x (results not shown) being recorded. The subsequent reaction of NO–O_2–C_8H_{18} at 198°C showed a negative peak in NO_x conversion due to NO_x desorption (Fig. 3a, Trace 3). Moreover, the initial *n*-octane conversion was also zero, indicating an absence of both De-NO_x and combustion activity. However, after the desorption of NO_x, reaction commenced, giving N_2, N_2O, and CO_2 as expected. The activity profile followed the same trend observed previously (Fig. 3, compare Traces 1 and 3), but the catalyst lifetime was approximately halved. This result indicates a dual effect for NO_2, as a site-blocking poison which is readily removed under reaction conditions, but also a more "toxic" effect which led to a loss in catalyst lifetime.

The second pretreatment in NO_2 resulted in a considerably larger adsorption of NO_2 (ca. 2.3×10^{-5} moles/g cat). In addition, the subsequent De-NO_x activity (Fig. 3, Trace 4) showed an initial large negative peak in NO_x conversion. Moreover, even after 100 min on-line both CO_2 production and NO_x conversion were strongly suppressed, clearly illustrating a severe poisoning.

These data may be contrasted with those of the cofed NO_2 case (Fig. 3, Traces 5a/5b), which showed a similar activity profile to the standard reaction. However, this sample exhibited a decrease in catalyst lifetime, confirming that excess NO_2 in the reaction mixture can influence the catalytic properties.

TABLE 2

Temperature-Programmed Oxidation and Desorption from 0.3% Pt/Al_2O_3 after *n*-C_8H_{18}–NO–O_2 Reactions

Prereaction[a]				NO_x desorption		CO_2 desorption	
Reductant	Temp (°C)	Time (h)	Technique	Amount (moles/$g_{cat} * 10^5$)	Peak (°C)	Amount (moles/$g_{cat} * 10^5$)	Peak (°C)
n-C_8H_{18}[b]	198	3	TPO	—	—	84	400
n-C_8H_{18}	198	3	TPO	2.3	375	107	375
n-C_8H_{18}	198	10	TPO	2.4	340	109	360/425
n-C_8H_{18}	198	3	TPD	—	—	17	450
n-C_8H_{18}	223	3	TPO	0.7	420	36	420
n-C_8H_{18}[c]	223	3	TPO	0.7	410	37	440
n-C_8H_{18}	223	10	TPO	1.4	400	45	440
C_3H_6	250	3	TPO	1.3	400	23	360/420
C_3H_6	250	10	TPO	2.9	400	64	400
n-C_8H_{18}[d]	198	3	TPO	2.5	400	110	350/420

[a] Prereaction 0.1 g clean 0.3% Pt/Al_2O_3 in 500 ppm NO/4000 ppm C/5% O_2 at total flow 200 $cm^3 min^{-1}$.
[b] Prereaction of 0.1 g clean 0.3% Pt/Al_2O_3 in 4000 ppm C/5% O_2, total flow 200 cm^3 min^{-1}.
[c] Catalyst deactivated at 198°C prior to 223°C reaction (see Fig. 2, Trace 2).
[d] Prereaction 0.1 g clean 0.3% Pt/Al_2O_3 in 480 ppm NO/20 ppm NO_2/4000 ppm C/5% O_2 at total flow 200 cm^3 min^{-1}.

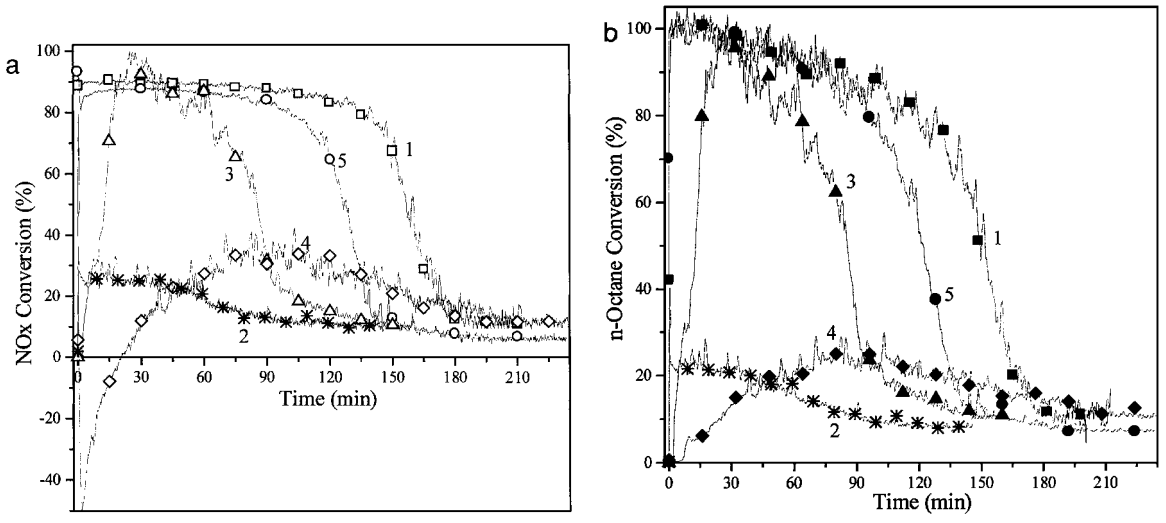

FIG. 3. Catalytic activity of 0.3% Pt/Al_2O_3 at 198°C. (a) NO_x conversion: (1) standard activity profile (see Fig. 2, Trace 2); (2, ∗) pretreated 198°C in n-C_8H_{18} (500 ppm)/O_2 (5%) for 3 h; (3, Δ) pretreated 198°C in NO (500 ppm) and O_2 (5%) in He for 1 h; (4, ◇) pretreated 198°C in NO_2 (420 ppm) and O_2 (5%) in He for 2 h; (5, ○) reaction of 500 ppm n-C_8H_{18}, 480 ppm of NO/20 ppm of NO_2, and 5% O_2 in He. (b) n-Octane conversion: (1, ■) standard activity; (2, ∗) pretreated 198°C in n-C_8H_{18} (500 ppm)/O_2 (5%) for 3 h; (3, ▲) pretreated 198°C in NO (500 ppm) and O_2 (5%) in He for 1 h; (4, ◆) pretreated 198°C in NO_2 (420 ppm) and O_2 (5%) in He for 2 h; (5, ●) reaction of 500 ppm n-C_8H_{18}, 480 ppm of NO/20 ppm of NO_2, and 5% O_2 in He.

(3) Microreactor Studies of the Activity and Deactivation of Supported 1% Pt catalysts

The De-NO_x reaction on a 1% Pt/Al_2O_3 catalyst was examined, and typical activity and product profiles versus temperature were obtained. This catalyst exhibited a significantly lower hydrocarbon light-off temperature, consistent with previous data (14, 18), and thus enabled us to examine isothermal activities at temperatures down to ca. 170°C (Fig. 4). It is clear, as previously observed, that small differences in temperature had dramatic effects upon activity and that the conversion of n-octane paralleled De-NO_x activity. Hence at 185°C, stable activity and >90% NO_x conversion were observed. In contrast, at 180°C high activity was only maintained for ca. 125 min. Rapid deactivation was more pronounced for reactions performed at 175 and 170°C (60 and ca. 6 min, respectively). In all cases it was found that catalyst bed temperature mirrored the state of activity or deactivation of the catalyst and that as deactivation commenced there was a concomitant decrease in catalyst temperature.

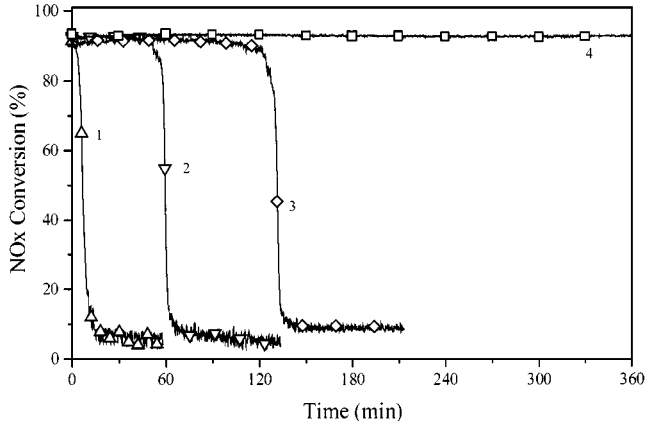

FIG. 4. De-NO_x activity isotherms of the n-C_8H_{18}–NO–O_2 reaction over 1%-Pt/Al_2O_3: (1, Δ) 170°C; (2, ∇) 175°C; (3, ◇) 180°C; (4, □) 185°C.

These deactivation data may be compared with those obtained for 0.3% Pt/Al_2O_3, 1% Pt/SiO_2, and 1% Pt/ZrO_2 catalysts. These results are summarised in Table 3. In all cases similar, characteristic activity/deactivation profiles were observed (detailed results not shown) with only the time scales at specific temperatures varying. Hence at 180°C, 1% Pt/ZrO_2 exhibited no deactivation, whilst 1% Pt/SiO_2 and 0.3% Pt/Al_2O_3 required temperatures of 190 and 223°C, respectively. However, it was found that the SiO_2-supported variant displayed extremely rapid deactivation at lower temperatures.

(4) TPO, TPD, and Related Activity Studies

Table 2 summarises the TPO and TPD results. From these data the following points emerge:

(a) TPO of 0.3% Pt/Al_2O_3 ex 198°C/3 h (Table 2, row 2) contains an organo-NO_x surface species, as indicated by coincidental CO_2/NO_x desorption peaks at 375°C, this simultaneous desorption being typical of the oxidative decomposition of a single species.

(b) TPD of a sample identical to (a) exhibited only a small CO_2 peak at 450°C (Table 2, row 4). However, GC analysis performed simultaneously with this desorption maximum confirmed the presence of N_2, CO, and multiple

TABLE 3

Isothermal Reaction Lifetime Data

Sample	Temperature (°C)	$T_{1/2}$ (min)[a]	T_{deact} (min)[b]
0.3% Pt/Al_2O_3	170	[c]	[c]
	180	7	13
	190	69	90
	198	161	180
	223	∞	∞
1% Pt/SiO_2	175	[c]	[c]
	180	[c]	[c]
	190	∞	∞
1% Pt/ZrO_2	170	36	41
	180	231	238
	185	∞	∞
1% Pt/Al_2O_3	170	7	13
	175	60	64
	180	132	136
1% Pt/Al_2O_3	170	12	15
Ex 700°C/15 h	175	81	83
	180	∞	∞
1% Pt/Al_2O_3	170	15	16
Ex 740°C/24 h	175	130	132
	180	∞	∞

Note. ∞ indicates no deactivation observed during lifetime of experiment (typically 6 h).

[a] Time taken for catalyst to deactivate to 50% of initial De-NO_x activity.

[b] Time for catalyst to exhibit NO_x conversion <10%.

[c] Unable to determine due to significant contribution of NO_x adsorption to activity.

organic fractions (but no N_2O) as desorbed species. These observations provide corroborative evidence for the presence of an organo-NO_{2ads} species undergoing decomposition and confirm that the NO_2 present was not formed from reaction between NO_{ads} and O_2 during the TPO. This is in agreement with Burch *et al.* (19), who show, for Al_2O_3, the amount of NO_{2ads} to be an order of magnitude greater than that of NO_{ads}, with a desorption maximum at ca. 425°C.

(c) Increasing the exposure of the 0.3% Pt/Al_2O_3 catalyst to the standard De-NO_x reaction mixture to 10 h shows no increase in the concentrations of surface deposits (Table 2, row 3). This indicates that after deactivation is complete, there is no further deposition of carbonaceous material. However, the desorption profiles obtained are different. The NO_x desorption maximum occurred at 340°C (cf. 375°C for the ex 3 h case), and the CO_2 desorption profile changed from a single to a multiple desorption phenomenon, the lower peak being broadly coincident with NO_x desorption.

(d) TPO of catalysts ex 223°C, where no deactivation occurred, showed lower levels of NO_x and CO_2, even after 10 h on-line (Table 2, rows 5 and 7). Moreover, the CO_2 desorption events were broader and at higher temperatures, indicating that the coke present was more tightly bound but present in lower quantities and of a less "poisonous" nature. It is also probable that the coke resides on the Al_2O_3, away from interfacial contact with Pt, and thus its removal is not facilitated by activated spillover species.

(e) TPO of the ex 198°C sample reactivated at 223°C showed similar trends evolving a quantity of CO_2 between those observed for the ex 198°C and ex 223°C samples, confirming desorption of organic material at higher reaction temperatures (Table 2, row 6). The higher peak maxima temperatures also suggested a more tightly bound CO_2 precursor, consistent with an "ageing" process.

(f) TPO of catalysts ex 250°C/C_3H_6–NO-O_2, which had displayed typical activity profiles (14, 16, 18) with no deactivation after 10 h, evolved markedly less CO_2 but comparable amounts of NO_x to that observed with the samples deactivated in *n*-octane (Table 2, rows 8 and 9).

(g) TPO of the ex NO_2 cofed sample (Fig. 3, Trace 4) exhibited dramatic differences in the CO_2 desorption profile with multiple desorption peaks identical to those observed for the ex 10 h/198°C case (Table 2, row 3).

(5) Adsorbate Pretreatment and FTIR Studies

TPO of adsorbed *n*-octane (Fig. 5a, Trace ◆) showed a broad, low-temperature phenomenon with a higher temperature shoulder and a smaller but equally broad high-temperature oxidation. Predosing with 500 ppm NO, 5% O_2 for 10 min at 198°C, and then treating with *n*-octane resulted in an immediate desorption of NO_x, even though the sample had been extensively purged, reflecting a competition between the hydrocarbon and the NO_x for adsorption sites. Subsequent TPO showed multiple peaks with CO_2 evolution exhibiting four peak maxima at ca. 150, 240, 370, and 480°C (Fig. 5a, Trace ◇) while NO_x maxima were noted at 250 and 380°C (Fig. 5b, Trace ◇) coincident with CO_2 peaks. The low-temperature CO_2 peak was ascribed to weakly adsorbed species which varied with purge, etc., while the high-temperature desorption CO_2 peak was ascribed to the "coke" observed previously.

Finally all three reagents were coadsorbed, i.e., reacted for 15 min and purged, and TPO was performed. This showed two CO_2 peaks, the low-temperature peak as before and a large desorption peak at 450°C (Fig. 5a, Trace ○), coincident with small NO_x peaks (Fig. 5b, Trace ○) reflecting the high conversion of NO_x to N_2/N_2O under dosing conditions. Similar results were found after the adsorption of a reagent mixture containing 20 ppm NO_2, except there was a large increase in the high-temperature CO_2 peak (Fig. 5a, Trace ●). These findings were supported by FTIR, which exhibited absorption peaks at ca. 3200 cm^{-1}, corresponding to δ C–H. Moreover, the presence of aromatic (Type II coke) bands (20) at 1586 cm^{-1} were noted. In addition, several very weak bands below 1500 cm^{-1} were recorded, which may indicate the presence of nitrite- (21), or nitrato- (22) type species.

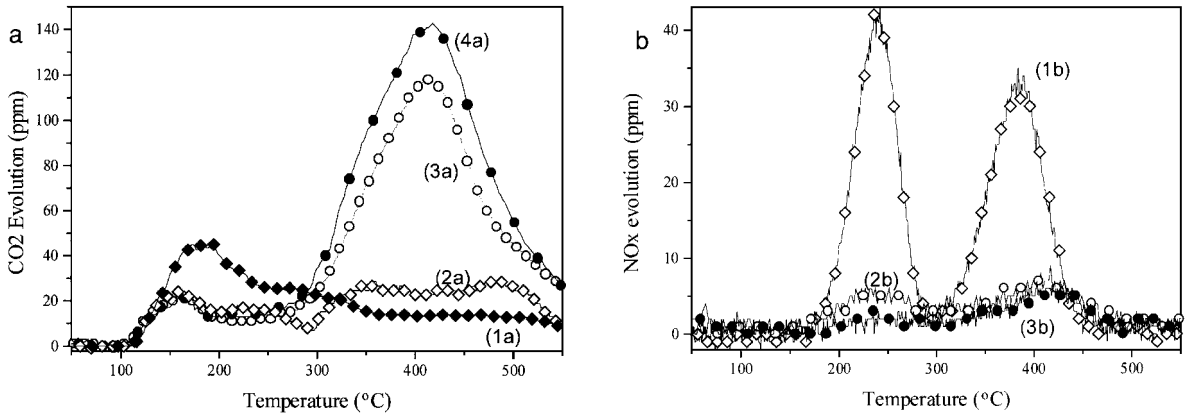

FIG. 5. TPO of adsorbates on "clean" Pt/Al_2O_3 at 198°C. (a) CO_2 evolution after adsorbing (1a, ◆) *n*-octane/10 min, (2a, ◇) *n*-octane + predosed NO (500 ppm)/O_2 (5%)/10 min at 198°C, (3a, ○) reaction feed/10 min, and (4a, ●) *n*-octane (500 ppm) NO (480 ppm) NO_2 (20 ppm) O_2 (5%). (b) NO_x evolution after adsorbing (1b, ◇) *n*-octane + predosed NO (500 ppm)/O_2 (5%)/10 min at the 198°C, (2b, ○) reaction feed/10 min, and (3b, ●) *n*-octane (500 ppm) NO (480 ppm) NO_2 (20 ppm) O_2 (5%).

(6) Effect of Metal Particle Size on Activity and Deactivation

Given that the isothermal lifetimes of fresh 1% Pt catalysts seemed to be related to Pt particle size ($Pt–ZrO_2 > Pt–Al_2O_3 \sim Pt–SiO_2$), the effect of sintering upon catalytic activity was examined. The isothermal lifetimes of 1% $Pt–Al_2O_3$ catalysts sintered under standard (15 h, 700°C, O_2/He) and vigorous (24 h, 740°C, O_2/He) conditions are detailed in Table 3. (Dispersions are given in Table 1.) It can be seen that the sintered catalysts exhibited improvements in lifetime at lower temperatures (cf. "fresh" 1% Pt case). At 180°C both samples exhibited high De-NO_x activity with no deactivation; cf. deactivation after ca. 130 min for the nonsintered case. The activity of the catalysts at 175 and 170°C was also enhanced.

(7) Effect of Temperature Spikes and Microinjections on Activity

The on-line reactivation of 0.3% Pt/Al_2O_3 in the 198/223°C experiment (Fig. 2, Traces 2 and 3) suggested the possibility of real-time reactivation of these catalysts. To test this, temperature spiking was employed. This entailed raising the furnace temperature rapidly from 198 to ≥230°C and then returning to 198°C. By this method it was found that complete reactivation of the catalyst was possible in real-time, with the total time of the temperature excursion being ca. 5 min.

As an alternative to this slow temperature excursion, we have attempted to create a similar thermal effect by injection into the standard reaction mixture small quantities of "thermal promoters," viz. combustible molecules. The combustion of these species would result in an exotherm, specifically localised at active Pt sites to promote the reaction or desorption of any deactivating residues located at or within the immediate vicinity of the active surface. H_2 and CH_3OH were selected as thermal promoters.

Figure 6 shows a comparison of the activities of 0.3% Pt/Al_2O_3 for the n-C_8H_{18}–O_2–NO reaction at 185°C, with and without microinjection. The data reveal no significant difference between the lifetimes of the standard 185°C reaction and when small amounts of H_2 are injected (Traces 1 and 2). Indeed, the only difference is the desorption of NO_x-containing species, concomitant with a bed exotherm of ca. 20°C, some 10 s after the H_2 injection. In contrast, an increase in lifetime of approximately 30 min was observed when larger, more regular pulses of H_2 were employed (Trace 3). Given the highly reproducible nature of the deactivation (which occurred within 60 s for different experiments performed under comparable conditions), this was a significant result. Again the reaction displayed a characteristic NO_x desorption and bed exotherm (ca. 30°C) after each injection of H_2.

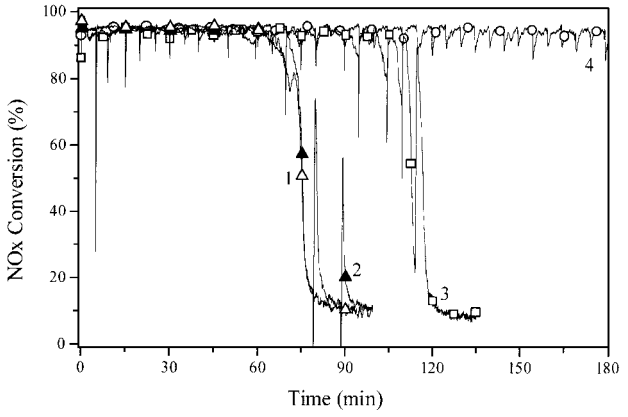

FIG. 6. The effect of H_2 and CH_3OH microinjections on the n-C_8H_{18}–NO–O_2 reaction at 185°C over 0.3% Pt/Al_2O_3: (1, Δ) no injection; (2, ▲) 0.5 cm^3 every 10 min; (3, □) 2 cm^3 every 5 min; (4, ○) 1 μl CH_3OH every 5 min.

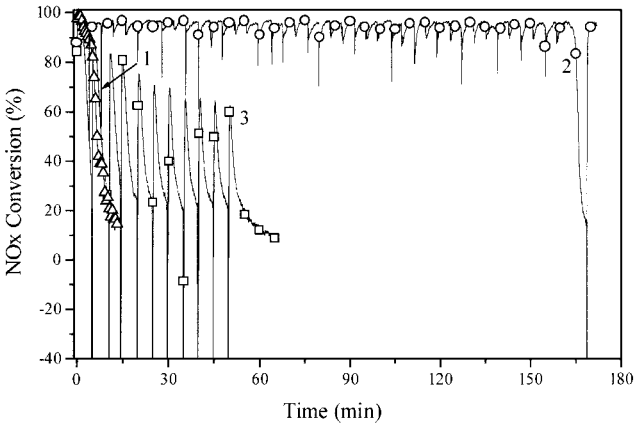

FIG. 7. The effect of CH_3OH microinjections on the *n*-C_8H_{18}–NO–O_2 reaction over 0.3% Pt/Al_2O_3 at 180°C: (1, Δ) no injection; (2, ○) 2 μl CH_3OH every 4 min; (3, □) activity of 2 μl CH_3OH pulses in absence of *n*-C_8H_{18}. Note after 160 min in trace 2, injections were ceased and then recommenced at 169 min.

The most dramatic results were obtained for CH_3OH injection (Trace 4). In this case there was no deactivation observed for >4 h on-line (the full lifetime is not reproduced in Fig. 6 to enhance clarity). It appears likely that by continued injection, deactivation could be completed avoided. Consistent with the observations for H_2, the CH_3OH injection was found to lead to the largest bed exotherm (with the in-bed temperature increasing some 40°C). Moreover it was found that in the initial stages of reaction there was a large desorption of NO_x, suggesting that the process of deactivation may be initiated very early in the life cycle of the catalyst.

Application of CH_3OH micropulsing at 180°C was also performed (Fig. 7). Previously, complete deactivation of 0.3% $Pt–Al_2O_3$ had been observed in ca. 6 min (Fig. 7, Trace 1) but by pulsing 2 μL of CH_3OH into the reaction every 4 min deactivation was avoided (Figure 7, Trace 2). Again catalyst bed temperature mirrored the state of the catalyst and reaction with bed temperatures increasing ca. 40–50°C some 12 s postinjection before decreasing to the "steady-state" temperature. After 160 min on-line with no deactivation, injection of CH_3OH was ceased and deactivation was found to occur in 6 min, in exact duplication of the response of the clean catalyst (Fig. 3, Trace 1). However at 169 min, CH_3OH injection was recommenced and the full activity of the catalyst recovered. These results confirm that the methanol effectively cleans the Pt surface to enable De-NO_x to occur.

This proposal is corroborated by analysis of the reaction of CH_3OH pulses in the absence of the *n*-octane feed (Fig. 7, Trace 3). In this case, whilst some De-NO_x activity was recorded, this decreased rapidly. In addition, upon introduction of each pulse of methanol there was a very large desorption of NO_x, indicating a significant contribution of adsorption to the apparent de-NO_x conversion measured. Finally, NO_x conversion as a function of the number of CH_3OH pulses introduced decreased, indicating a low steady-state conversion with methanol. Thus it is clear that the enhanced stability in the octane De-NO_x reaction is not due to methanol acting as the primary reductant. This is consistent with the results of Engler *et al.* (18), who observed combustion of CH_3OH at >150°C, but with <10% NO_x conversion, and Halpin (24), who observed a maximum NO_x conversion of ca. 50% using a comparable 0.3% $Pt–Al_2O_3/CH_3OH–NO–O_2$ system, but only at $T > 250$°C.

4. DISCUSSION

(1) Activity and Deactivation of Pt-Based De-NO_x Catalysts

The results obtained in this study reflect the highly complex nature of the De-NO_x reaction and the delicately balanced surface chemistry of the catalyst. In an attempt to rationalise the observations in this study and elsewhere we shall address the various factors which contribute to activity or deactivation.

(i) Chemical factors. While it is self-evident that reactivity is primarily influenced by surface intermediate concentrations the results obtained indicate that any perturbation of the "normal equilibrium" regime has negative consequences. Thus exposure of the catalyst to reaction mixture at low temperatures (Fig. 2, Trace 1), pretreatment in *n*-octane/O_2 (Fig. 3, Trace 2), or pretreatment with NO_2 (Fig. 3, Trace 4) all resulted in a loss of activity. Conversely, pretreatment with NO/O_2 or NO_2 cofeeding (Fig. 3, Traces 3 and 5 respectively) led to a reduction in catalyst lifetime. These differences in the activity of clean and pretreated surfaces highlight the importance of the surface chemistry and the competition for surface sites, e.g., *n*-octane displacement of $Pt–NO_{x\text{ads}}$, between the various species.

The shape of the deactivation profiles indicates that under reaction conditions there is a formation and accumulation of deposits that at a specific threshold point results in site blockage and rapid deactivation. The presence of multiple GC elution peaks and shifts in the position of the high-temperature CO_2 peak in TPO further suggests the presence of multiple "coke" species or an "ageing" of deposits as suggested by Karge *et al.* (20). Thus it is proposed that deactivation is a function of concentration, type, and particularly location of retained species, as reflected in TPO/TPR CO_2 evolution profiles. These show decreasing CO_2 production with increasing De-NO_x reaction temperature but an increasing temperature required for oxidation of the deposits. This indicates more tightly bound moieties removed from the immediate vicinity of any Pt particles where activated spillover oxygen would facilitate their combustion, i.e., increasingly "benign" deposition removed from the active sites.

The identity of these moieties is unclear, but in addition to TP evidence, FTIR further suggests the presence of an aromatic/H deficient hydrocarbon (Type II coke bands at 1586 cm^{-1} (20)). TPR/TPO also indicates that these species are at least adjacent to, and possibly formally complexed with, NO_{xads} (as nitrate/nitrato ONO_2 (21–23)), hence explaining the ability of the latter to initiate combustion. We propose that this is an organo-NO_x species adsorbed on Al_2O_3 and may correspond to the various N–C–O-containing variants cited elsewhere (24–27). Such species are unlikely to be directly responsible for deactivation, given their isolation for the Pt, but their presence may be contributory due to encroachment, particularly at lower De-NO_x reaction temperatures. Thus the absolute quantity of deposition necessary for deactivation varies for the different catalysts, as reflected in the results of this study. Moreover, since deactivation arises due to deposition on the Pt, it is apparent that both the absolute loading of Pt and the size of the individual Pt particles are determining factors with respect to this phenomenon.

The situation may be further complicated by the characteristics of the support. For example, for a noninteracting support, such as SiO_2, deactivation in the lower temperature regimes is extremely rapid. This may be due to the low inherent activity of SiO_2 toward hydrocarbon oxidation. Hence reaction can only proceed on the free Pt surface. In contrast, ZrO_2 and Al_2O_3 may be considered to be interactive supports and display a degree of reactivity toward hydrocarbon activation (33–36). Thus these materials may exhibit a higher tolerance to deactivation due to their ability to facilitate reaction of the retained hydrocarbonaceous or organo-NO_x species in the vicinity of the Pt/support interface.

(ii) Catalyst temperature and thermal effects. The highly exothermic nature of the combustion reaction, as reflected in the large bed exotherms (up to 60°C), means that the balance between energy input and energy release is an important factor. All the results obtained in this study, and in particular for the microinjection experiments, show that the bed exotherm and stability for the De-NO_x reaction are inextricably linked, and the decline of one is concomitant with a loss of the other. Indeed, it is probable that the measured exotherm reflects an even larger temperature effect at the individual Pt particles where the exotherm is created by the combustion reaction. This is a general phenomenon and is accommodated into an overall reaction rate for a catalyst operating at steady state.

However, our experiments show that there are critical temperatures where the catalysts can appear to be at steady state but after a period of time, varying from a few minutes to several hours, suddenly deactivate. We think this is closely related to the balance between the rate of adsorption and the rate of removal of carbon-containing material, which, in turn, is critically dependent on the precise temperature of the Pt particles. A small increase in the coverage of the Pt with carbon can cause a small decrease in the rate of combustion, which leads to a small decrease in the temperature of the Pt. Further cycling through these stages can soon result in a very severe deactivation of a catalyst which was apparently at steady state and highly active. The presence of NO_2, or NO_2 cofeeding, exacerbates this phenomenon with coadsorbed NO_2 facilitating both further *n*-octane adsorption upon an already "coked" site, through adsorbate assisted interaction, as proposed by Burch *et al.* (19, 24) and also "excess" hydrogen abstraction from adsorbates already present (30, 31). This would to lead to the formation of graphitic carbon species which would be more difficult to combust, consistent with the high-temperature CO_2 peak in TPO (Fig. 5a, Traces ○ and ●), thus accelerating deactivation. The presence of NO_2-derived species on reduced/coked Pt is supported by the results of the microinjection experiments which displayed simultaneous CO_2 and NO_x evolution.

(iii) Particle size effect. The increased tolerance to deactivation exhibited by sintered 1% Pt/Al_2O_3 catalysts indicates that Pt particle size is a key factor in low-temperature De-NO_x. This is in contrast to work on hydrocarbon combustion (33–35) which indicates that small particles are more active. However, it is consistent with the findings of Kašpar *et al.* (39), who have shown that small metal particles are less able to facilitate NO dissociation. In addition, Otto and Yao (40) have shown that particulate Pt is more active than dispersed Pt, again by increasing NO dissociation probability. Moreover, Demicheli *et al.* (41) and Burch and Millington (14) have reported increases in specific reaction rates/turnover frequencies with increased Pt particle size. Thus it seems likely that a combination of enhanced surface reactivity and deactivation tolerance both contribute to the enhanced stability of the sintered catalysts.

In summary we ascribe the process of deactivation to the formation of hydrocarbonaceous deposits which may include organonitrogen species. This material gradually accumulates in the immediate vicinity of the active Pt particles (Pt/support interface). This results in a slow but progressive buildup in the coverage of the Pt with deposits which inhibit the combustion and De-NO_x reactions. The combustion exotherm is thus diminished, and the Pt particles cool somewhat, resulting in a further increase in the rate of deposition of the carbon-containing material. Continuation of this cycle ultimately leads to severely deactivated catalysts.

(2) In Situ, Real-Time Regeneration

Attempts to regenerate catalysts on-line were generally successful and provided further corroboration for the proposed mechanism of deactivation. In both temperature "spiking" and microinjection protocols the pivotal role of reaction temperature on the balance of the reaction is confirmed.

A comparison of the effects of H_2, CH_3OH, or *n*-octane illustrates that while the former molecules were able to facilitate regeneration, the latter was only able to result in

short bursts of enhanced activity. However, CH_3OH is superior to hydrogen when used at comparable molar levels (ca. 10^{-5} mol). This is ascribed to the significantly higher molar enthalpy of combustion for methanol (-285.8 for H_2; cf. -715.0 kJ mol^{-1} for CH_3OH (42)).

The cleaning process itself appears to be due to the oxidation/desorption of the carbon-containing material referred to above. This is shown in the twin observations of a combustion spike and an NO_x desorption peak (Figs. 6 and 7). The extent of the combustion exotherm was found to be larger on average in the *n*-octane + CH_3OH pulse than in the CH_3OH pulse only (Fig. 7, Traces 2 and 3, respectively). This clearly indicates that in addition to the combustion of the CH_3OH there was a concomitant combustion of a secondary species on the Pt which contributed to the total exotherm.

5. CONCLUSIONS

Supported Pt catalysts possess high, but metastable, activity for the reduction of NO_x under lean burn conditions using *n*-octane as a reductant at temperatures below the hydrocarbon light-off provided an initially clean Pt surface is employed. Pretreatment of the surface by *n*-octane/O_2, NO/O_2, or NO_2 has deleterious effects on catalyst activity and/or lifetime. De-NO_x activity is intrinsically linked to combustion, as shown by the observation of the bed exotherm and the CO_2 production declining prior to De-NO_x deactivation. Deactivation is ascribed to the deposition of carbon-containing material which leads to a decrease in the actual temperature of the individual Pt particles. Once the temperature falls below a critical value, very rapid deactivation occurs, probably due to the further coverage of the Pt. Deactivation thus arises due to a negative feedback loop involving inhibition of hydrocarbon combustion and desorption processes. The use of catalysts containing larger Pt particles enhances NO_x conversions at comparatively low temperatures.

Stable De-NO_x activity has been demonstrated at low temperatures by pulsing small quantities of CH_3OH as a "thermal" promoter. This appears to facilitate desorption/reaction of deactivating residues and returns the catalyst surface to an active state.

ACKNOWLEDGMENTS

We are grateful for financial support for this work through EU Grant EV5V-CT94-0535. We also acknowledge Dr. James Sullivan for helpful discussions, Johnson Matthey for the supply of Pt salts, and Akzo for providing the Al_2O_3 support and 0.3% Pt/Al_2O_3 catalyst.

REFERENCES

1. Adams, K. M., Cavataio, J. V., and Hammerle, R. H., *Appl. Catal. B* **10**, 157 (1996).
2. Frost, J. C., and Smedler, G. S., *Catal. Today* **26**, 207 (1995).
3. Taylor, K. C., *Catal. Sci. Technol.*, 5 (1984).
4. Iwamoto, M., Furukawa, H., Mine, Y., Mikuriya, S., and Kagawa, S., *J. Chem. Soc. Chem. Commun.*, 1272 (1986).
5. Iwamoto, M., Yahiro, H., Tanda, K., Mizuno, N., Mine, Y., and Kagawa, S., *J. Phys. Chem.* **95**, 3727 (1991).
6. Burch, R., and Millington, P. J., *Appl. Catal. B* **2**, 101 (1993).
7. Walker, A. P., *Catal. Today* **26**, 107 (1995).
8. Armor, J. N., *Catal. Today* **26**, 147 (1995).
9. Tanaka, T., Iijima, T., Koiwai, A., Mizuno, J., Yokota, K., and Isogai, A., *Appl. Catal. B* **6**, 145 (1995).
10. Kucherov, A. V., Hubbard, C. P., and Shelef, M., *J. Catal.* **157**, 275 (1995).
11. Kharas, K., Robota, H. J., and Liu, D. J., *Appl. Catal. B* **2**, 225 (1993).
12. Fritz, A., and Pitchon, V., *Appl. Catal. B* **13**, 1 (1997).
13. Shin, H. K., Hirabayshi, H., Yahiro, H., Wanatabe, M., and Iwamoto, M., *Catal. Today* **26**, 13 (1995).
14. Burch, R., and Millington, P. J., *Catal. Today* **26**, 185 (1995).
15. Zhang, G., Yamaguchi, T., Kawakami, H., and Suzuki, T., *Appl. Catal. B* **1**, L1 (1993).
16. Burch, R., and Watling, T. C., *Catal. Lett.* **43**, 19 (1997).
17. Burch, R., Millington, P. J., and Walker, A. P., *Appl. Catal. B* **4**, 65 (1994).
18. Engler, B. H., Leyrer, J., Lox, E. S., and Ostgathe, K., *in* "Third International Congress on Catalysis and Automotive Pollution Control, Brussels" (A. Frenner and J. M. Bastin, Eds.), Vol. 1, p. 2109. 1994.
19. Burch, R., Halpin, E., and Sullivan, J. A., *Appl. Catal. B* **17**, 115 (1998).
20. Karge, H. G., Niessen, W., and Bludau, H., *Appl. Catal. A* **146**, 339 (1996).
21. Arai, H., and Tominga, H., *J. Catal.* **43**, 131 (1976).
22. Hoost, T. E., Otto, K., and La Fromboise, K. A., *J. Catal.* **155**, 303 (1995).
23. Hierl, R., Urbach, H.-P., and Knozinger, H., *J. Chem. Soc. Faraday Trans.* **88**, 355 (1992).
24. Halpin, E., Ph.D. thesis, University of Reading. 1998.
25. Tanaka, T., Okuhura, T., and Misono, M., *Appl. Catal. B* **4**, L1 (1994).
26. Li, C., Bethke, K. A., Kung, H. H., and Kung, M. C., *J. Chem. Soc. Chem. Commun.*, 813 (1995).
27. Bell, V. A., Feeley, J. S., Deeba, M., and Farrauto, R. J., *Catal. Lett.* **29**, 15 (1994).
28. Hamada, H., *Catal. Today* **22**, 21 (1994).
29. Obuchi, A., Nakamura, M., Ogata, A., Mizuno, K., Ohi, A., and Obuchi, H., *J. Chem. Soc. Chem. Commun.*, 1150 (1992).
30. Petunchi, J. O., and Hall, W. K., *Appl. Catal. B* **2**, L17 (1993).
31. Bethke, K. A., Li, C., Kung, M. C., Yang, B., and Kung, H. H., *Catal. Lett.* **29**, 29 (1994).
32. d'Itri, J. L., and Sachtler, W. M. H., *Appl. Catal. B* **2**, 7 (1993).
33. Hubbard, C. P., Otto, K., Gandhi, H. S., and Ng, K. S., *J. Catal.* **139**, 268 (1993).
34. Burch, R., and Hayes, M. J., *J. Mol. Catal. A* **100**, 13 (1995).
35. Burch, R., and Loader, P. K., *Appl. Catal. A* **143**, 317 (1996).
36. Igarashi, A., Ohtaka, T., Homma, T., and Fukuhara, C., *in* "New Frontiers in Catalysis" (L. Guczi *et al.*, Eds.), p. 2083. Elsevier, Amsterdam, 1993.
37. Burch, R., Fornasiero, P., and Watling, T. C., *J. Catal.* **176**, 204 (1998).
38. Inaba, M., Kintaichi, Y., and Hamada, H., *Catal. Lett.* **36**, 223 (1996).
39. Kašpar, J., de Leitenberg, C., Fornasiero, P., Trovarelli, A., and Graziani, M., *J. Catal.* **146**, 136 (1994).
40. Otto, K., and Yao, H. C., *J. Catal.* **66**, 229 (1980).
41. Demicheli, M. C., Hoang, L. C., Menezo, J. C., Barbier, J., and Pinabiaucarlier, M., *Appl. Catal. A* **97**, L11 (1993).
42. Stark, J. G., and Wallace, H. G., Eds., "Chemistry Data Book," 2nd ed. Murray, London, 1982.